11. Motta-Hennessy C, Sharkey RM, Goldenberg DM. Metabolism of indium-111-labeled murine monoclonal antibody in tumor and normal tissue of the athymic mouse. *J Nucl Med* 1990;31:1510–1519.
12. Shih LB, Thorpe SR, Griffiths GL, et al. The processing and fate of antibodies and their radiolabels bound to the surface of tumor cells in vitro: a comparison of nine radiolabels. *J Nucl Med* 1994;35:899–908.
13. Zalutsky MR, Noska MA, Colapinto EV, Garg PK, Bigner DD. Enhanced tumor localization and in vivo stability of a monoclonal antibody radioiodinated using N-succinimidyl 3-(tri-n-butylstannyl)benzoate. *Cancer Res* 1989;49:5543–5549.
14. Wilbur DS, Hadley SW, Hylarides MD, et al. Development of a stable radioiodinating reagent to label monoclonal antibodies for radiotherapy of cancer. *J Nucl Med* 1989;30:216–226.
15. Ali SA, Warren SD, Richter KY, et al. Improving the tumor retention of radioiodinated antibody: aryl carbohydrate adducts. *Cancer Res* 1990;50:(suppl):783s–788s.
16. Stein R, Goldenberg DM, Thorpe SR, Mattes MJ. Effects of radiolabeling monoclonal antibodies with a residualizing iodine radiolabel on the accretion of radioisotope in tumors. *Cancer Res* 1995;55:3132–3139.
17. Reist CJ, Archer GE, Kurpad SN, et al. Tumor-specific anti-epidermal growth factor receptor variant III monoclonal antibodies: use of the tyramine-cellobiose radioiodination method enhances cellular retention and uptake in tumor xenografts. *Cancer Res* 1995;55:4375–4382.
18. Stein R, Basu A, Chen S, Shih LB, Goldenberg DM. Specificity and properties of MAb RS7–3G11 and the antigen defined by this pancarcinoma monoclonal antibody. *Int J Cancer* 1993;55:1–9.
19. De Leij L, Helfrich W, Stein R, Mattes MJ. SCLC-Cluster-2 antibodies detect the pancarcinoma/epithelial glycoprotein EGP-2. *Int J Cancer* 1994;8:(suppl):60–63.
20. Huet C, Ash JF, Singer SJ. The antibody-induced clustering and endocytosis of HLA antigens on cultured human fibroblasts. *Cell* 1980;21:429–438.
21. Stein R, Chen S, Sharkey RM, Goldenberg DM. Murine monoclonal antibodies raised against human non-small cell carcinoma of the lung: specificity and tumor targeting. *Cancer Res* 1990;50:1330–1336.
22. Siegel JA, Stabin MG. Absorbed fractions for electrons and beta particles in small spheres [Abstract]. *J Nucl Med* 1988;29:803.
23. Ong GL, Mattes MJ. Penetration and binding of antibodies in experimental human solid tumors grown in mice. *Cancer Res* 1989;49:4264–4273.
24. Fenwick JR, Philpott GW, Connett JM. Biodistribution and histological localization of anti-human colon cancer monoclonal antibody (MAb) 1A3: the influence of administered MAb dose on tumor uptake. *Int J Cancer* 1989;44:1017–1027.
25. Blumenthal RD, Fand I, Sharkey RM, Boerman OC, Kashi R, Goldenberg DM. The effect of antibody protein dose on the uniformity of tumor distribution of radioantibodies: an autoradiographic study. *Cancer Immunol Immunother* 1991;33:351–358.
26. Juweid M, Neumann R, Paik C, et al. Micropharmacology of monoclonal antibodies in solid tumors: direct experimental evidence for a binding site barrier. *Cancer Res* 1992;52:5144–5153.
27. Stein R, Blumenthal R, Sharkey RM, Goldenberg DM. Comparative biodistribution and radioimmunotherapy of monoclonal antibody RS7 and its Fab'_2 in nude mice bearing human tumor xenografts. *Cancer* 1994;73:816–823.
28. Stein R, Chen S, Sharkey RM, Goldenberg DM. Radioimmunotherapy of human non-small cell carcinoma of the lung xenografts with ^{131}I-labeled monoclonal antibody RS7–3G11. *Antibody Immunoconj Radiopharm* 1991;4:703–712.
29. Schlom J, Siler K, Milenic D, et al. Monoclonal antibody-based therapy of a human tumor xenograft with a ^{177}Lu-labeled immunoconjugate. *Cancer Res* 1991;51:2889–2896.
30. Strobel JL, Baynes JW, Thorpe SR. Iodine-125-glycoconjugate labels for identifying sites of protein catabolism in vivo: effect of structure and chemistry of coupling to protein on label entrapment in cells after protein degradation. *Arch Biochem Biophys* 1985;240:635–645.

Pharmacokinetics and Experimental PET Imaging of a Bromine-76-Labeled Monoclonal Anti-CEA Antibody

Anna Lövqvist, Anders Sundin, Håkan Ahlström, Jörgen Carlsson and Hans Lundqvist
Biomedical Radiation Sciences, University PET Center and Department of Diagnostic Radiology, Uppsala University, Uppsala, Sweden

Bromine-76 is potentially useful as a radiolabel for monoclonal antibodies (MAbs) in PET imaging. The purpose of the present study was to evaluate the ^{76}Br-labeled anticarcinoembryonic antigen (-CEA) MAb 38S1 as a tumor imaging agent in an experimental tumor model and to study the pharmacokinetics of ^{76}Br-38S1 in comparison with ^{125}I-38S1. **Methods:** Nude rats carrying human colon carcinoma xenografts were co-injected with directly labeled ^{76}Br-38S1 and ^{125}I-38S1. Biodistribution of labeled 38S1 was monitored for 4 days after administration, in the case of ^{76}Br activity, including PET imaging. In addition, catabolism of radiolabeled MAbs was analyzed by gel filtration chromatography of blood plasma and homogenized tissues. **Results:** Tumor sites could be readily identified by PET imaging from 46 hr after administration of ^{76}Br-38S1 and onwards. The concentration of ^{76}Br activity in tumors, blood and most normal tissues was higher than the corresponding ^{125}I concentration at all time points. This was mainly due to catabolism of radiolabeled MAb, resulting in free radiohalides, of which $^{76}Br^-$ was retained in contrast to the rapidly excreted $^{125}I^-$ ion. **Conclusion:** Bromine-76-labeled anti-CEA MAbs may be applied for experimental tumor imaging with PET.

Key Words: bromine-76; MAbs; PET; radioimmuno PET

J Nucl Med 1997; 38:395–401

For the imaging of monoclonal antibodies (MAbs) using PET, the choice of radiolabel is of major importance. The PET technique offers a higher resolution than SPECT and also allows radionuclide quantification with high accuracy. However, the production and use of suitable positron-emitting radionuclides for this purpose are less well-established than those of the standard SPECT radionuclides.

The physical half-life of a positron emitter in relation to the pharmacokinetics of the selected antibody and the labeling methods available for each nuclide are examples of factors determining the choice of radionuclide. Short-lived positron-emitters such as the routinely available PET nuclide ^{18}F ($T_{1/2}$ 110 min) have been used as radiolabels for rapidly clearing MAb fragments (*1–4*), whereas intact MAbs require radionuclides with longer half-lives, such as ^{66}Ga ($T_{1/2}$ 9.4 hr) (*5*), ^{64}Cu ($T_{1/2}$ 13 hr) (*6*), ^{76}Br ($T_{1/2}$ 16 hr) (*7*), ^{55}Co ($T_{1/2}$ 18 hr) (*8*) and ^{124}I ($T_{1/2}$ 4 days) (*9–15*).

To date, ^{124}I has been the nuclide most extensively utilized for clinical and experimental radioimmuno PET. However, the decay properties of ^{124}I are not ideal for PET imaging purposes since the positron abundance is only 23%. Combined with the long physical half-life, this may result in unnecessarily high patient radiation doses. In the halogen group, the only other positron emitter potentially useful for labeling of intact MAbs is ^{76}Br (Table 1), which was previously used mainly for labeling of various receptor ligands (*16*). The majority of the positrons emitted in the ^{76}Br decay have a high maximum energy (3.4 MeV) which affects both image resolution and radiation dose, but 55% of the decays do result in positron emission. As a radiolabel for radioimmuno PET, ^{76}Br is therefore an interesting alternative to ^{124}I.

Similar principles may be applied for direct bromination as for iodination of proteins, i.e., oxidation of the halide, although a more powerful oxidant may be required for sufficient yield in

Received Feb. 26, 1996; revision accepted Jun. 13, 1996.
For correspondence or reprints contact: Anna Lövqvist, PhD, Biomedical Radiation Sciences, Uppsala University, Box 535, S-751 21 Uppsala, Sweden.

TABLE 1
Decay Scheme of Bromine-76

Half-life (hr)	Decay mode (% Branching ratio)	β^+_{max}-energies (% Abundance)	Main photon energies (% Abundance)
16.2	β^+ (55)	3.4 MeV (26)	511 keV (110)
		871 keV (6.0)	
	EC (45)*	3.9 MeV (6.3)	559 keV (74)
		990 keV (5.2)	1.85 MeV (15)

EC = electron capture.

the labeling reaction. An enzymatic method for the radiobromination of proteins under mild reaction conditions that results mainly in labeled tyrosine residues (*17*), as with oxidative radioiodination techniques, was developed by McElvany and Welch (*18*). This method has been applied for radiobromine labeling of MAbs with preserved immunoreactivity (*7,19*).

The purpose of the present investigation was to evaluate the potential of the ^{76}Br-labeled anti-CEA MAb 38S1 for PET imaging of experimental tumors. The tumor uptake, pharmacokinetics and catabolism of the ^{76}Br-labeled anti-CEA MAb 38S1 was compared with ^{125}I-38S1, previously used for radioimmuno localization in rats with subcutaneous xenografts of human colonic cancer (*20,21*). For control purposes, the biodistribution of an irrelevant MAb labeled with either ^{76}Br or ^{125}I, as well as the radiohalides $^{76}Br^-$ and $^{125}I^-$ was also investigated.

MATERIALS AND METHODS

MAb 38S1

MAb 38S1, a mouse anti-CEA antibody of the IgG1-κ isotype, and a nonspecific MAb of the same IgG type, 79C, were kindly donated by Pharmacia, Uppsala, Sweden (*22*). A partially purified preparation of bromoperoxidase (10% protein, 9 units/mg solid) and iodotyrosine were used. Bromotyrosine, synthesized according to De Jesus et al. (*23*), was kindly provided by Stefan Sjöberg, Uppsala University. Sodium bromide and sodium iodide were from commercial sources. Sephadex G-25 desalting columns (NAP-5 and PD10), FPLC gel filtration columns (Superdex 200 HR 10/30) and NHS-activated columns (HITRAP) were from Pharmacia. For high-performance liquid chromatography, a Beckman 126 pump and 166 UV detector, a detector for beta radiation and a FRAC 100 fraction collector (Pharmacia) were used. The PET tomograph consisted of eight rings, which allowed examination of a 10 cm region, producing 15 slices. Bromine-76 was produced using the ^{nat}Br(p,xn)^{76}Kr, ^{76}Kr → ^{76}Br reaction (*24*). Iodine-125, in the form of sodium iodide, was purchased from Amersham International, Buckhamshire, England.

Radiolabeling

Bromine-76-Labeling. 100 μg MAb 38S1 was mixed with 70–85 MBq ^{76}Br preparation and 0.6 units bromoperoxidase (BPO) in 300 μl 50 m*M* phosphate buffer, pH 7.0, containing 80 μ*M* H_2O_2 (*7*). After 30 min incubation at 0°C, the reaction was terminated by adding sodium metabisulphite (final concentration 1.7 m*M*) and radiobrominated protein separated from free radiobromide on a NAP-5 column. Brominated antibodies were purified from the BPO preparation by affinity chromatography, using CEA coupled to an NHS-activated HITRAP column. Antigen-bound ^{76}Br-38S1 MAbs were eluted in 3 *M* NH_4SCN and immediately applied on a PD-10 column for buffer exchange to 50 m*M* phosphate-buffered saline (PBS), pH 7.4. MAb 79C was ^{76}Br-labeled using a similar protocol, but the amount of ^{76}Br used in the labeling reaction was only 19 MBq, and no affinity purification was performed. The radiochemical purity of this ^{76}Br-79C preparation was considered satisfactory, since only a minor amount of the bromoperoxidase preparation was labeled in the presence of excess amounts of MAb 79C, as analyzed on a Superdex 200 HR column.

Iodine-125-Labeling. The chloramine-T method was applied for radioiodination. Seventy micrograms MAb 38S1 or 79C was mixed with 18.5 MBq ^{125}I and 10 μg chloramine-T in 50 μl 0.05 *M* phosphate buffer, pH 7.5. After incubation for 10 min at 0°C, sodium metabisulphite was added to a final concentration of 1.7 m*M*, and ^{125}I-38S1 separated from unreacted ^{125}I on a NAP-5 column.

The proportion of ^{76}Br-labeled and ^{125}I-labeled 38S1 MAbs bound at equilibrium to excess amounts of CEA, covalently coupled to paper disks, was used as a measure of immunoreactivity for labeled 38S1.

In Vitro Stability

Duplicate samples of ^{76}Br-38S1 and ^{125}I-38S1 preparations were incubated at 37°C in blood plasma from nontumor-bearing rats. During 4 days of incubation, samples were taken once a day for separation on PD-10 columns into high and low molecular weight fractions, which were analyzed by gamma counting.

Tumor Model

Nude rats (Rowett nu/nu, The Wallenberg Laboratory, Lund, or Uppsala Biomedical Center, Uppsala, Sweden), housed in a controlled environment and fed ad libitum, were used. For anesthesia, chloral hydrate (36 mg/100 g body weight) was administered intraperitoneally. 6×10^6 LS174T human colonic adenocarcinoma cells (*25*) in 150 μl were injected subcutaneously into the left hind leg and right flank of 27 rats. At the time of radioimmuno localization experiments, initiated 12–14 days after tumor cell injections, the rats weighed between 200 and 274 g, and tumors had developed at all but one injection site. The ^{125}I uptake in thyroid glands had been suppressed by adding potassium iodide to the drinking water 24 hr before radiotracer injection. The rats were killed by exsanguination under anesthesia. Tumors weighed between 10 mg and 3.7 g (average 0.98 g).

In Vivo Distribution and Catabolism

Biodistribution. A double label technique was applied. Fifteen rats were injected intravenously with a mixture of ^{76}Br-38S1 and ^{125}I-38S1, 2–3 MBq and 0.01 mg of each. Nine rats were injected with free $^{76}Br^-$ and $^{125}I^-$, 4 and 2 MBq, respectively. At various time points after administration, blood samples were drawn from a tail vein from the remaining animals and three rats at each time point killed and dissected. Three rats were injected with 0.5 MBq ^{76}Br-79C and 2 MBq ^{125}I-79C, 0.01 mg of each, and killed and dissected 92 hr after administration. Blood was drawn from the heart, and tumors and pieces of normal tissues were weighed and measured for radioactivity in a well scintillation NaI(Tl) detector. All well-counter measurements were corrected for background contribution of ^{76}Br in the ^{125}I window and for radioactive decay. Accumulation index (AI) was calculated as (tissue radioactivity/tissue weight)/(injected radioactivity/body weight). AI is equivalent to the PET unit standardized uptake value (see below), approximating tissue density to 1 g/ml.

Catabolism. Samples of dissected tumors, kidneys and livers were homogenized in 2 ml cold saline, and homogenates and heparinized blood centrifugated for 10 min at 2500 rpm. The radioactivity in the supernatant and in the pellet was measured, after which the supernatant was analyzed by both low-pressure and FPLC gel filtration. 500 μl was applied on a PD-10 column, and separated in high (HMW, >5 kD) and low (LMW, <5 kD) molecular weight fractions. The proportion of ^{76}Br or ^{125}I activity after PD 10 fractionation (pellet, HMW, LMW) was correlated to the accumulation index of ^{76}Br or ^{125}I in the whole tissue sample.

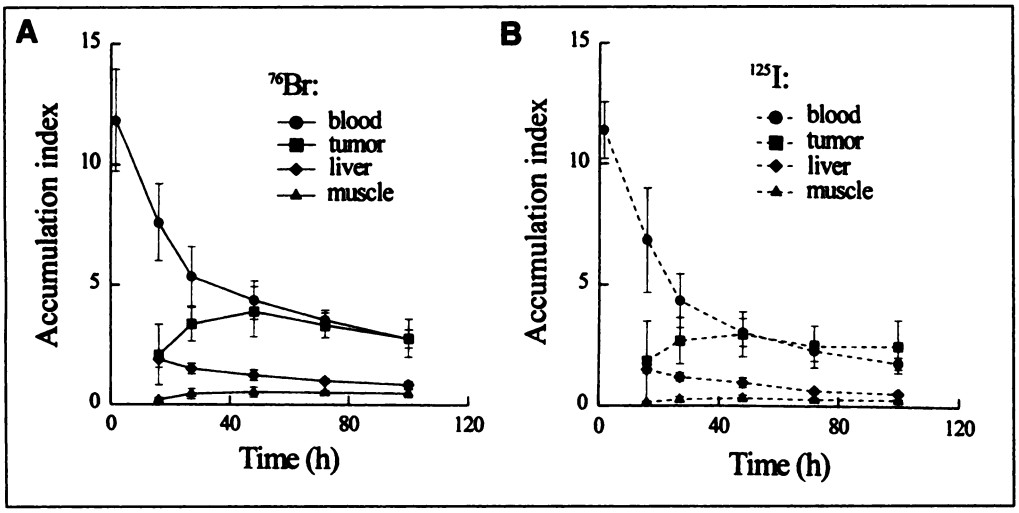

FIGURE 1. Accumulation index of ^{76}Br (A) and ^{125}I (B) over time for ^{125}I-labeled and ^{76}Br-labeled MAb 38S1. Blood samples (circles) were taken from 3–15 rats. Samples from tumors (squares), liver (diamonds) and muscle (triangles) were taken from three rats at each time point.

After filtration through a low protein binding 0.2 μm filter, 200 μl supernatant was applied on a Superdex 200 HR column coupled to an HPLC system, using 1 ml/min 50 m*M* PBS as the eluent. Fractions were collected (1 min/fraction) and measured for radioactivity. Reference compounds were analyzed in the same system by UV-spectroscopy and radioactivity measurements, including unlabeled, ^{76}Br-, ^{125}I-labeled 38S1 (UV 280 nm), iodo- and bromotyrosine (UV 254 nm), radioiodide and radiobromide, as well as nonradioactive iodide and bromide (UV 210 nm).

PET Imaging

At 25, 46 and 65 hr after administration of radiolabeled MAb 38S1, the remaining rats were anesthetized and placed prone in the gantry in a multicompartment holder enabling simultaneous examination of seven animals. After transmission scans (attenuation correction) and subtraction scans (correction of transmission scans for injected radioactivity), emission data were collected during 45–60 min. In the transaxial images, radioactivity concentration was measured in circular regions of interest (ROIs) over the tumors (1.0 cm^2) and the liver (3.5 cm^2). After decay correction of these measurements, the standard uptake value (SUV), defined as (radioactivity/ml)/(injected radioactivity/g body weight), was calculated. With a tissue density of 1 g/ml, the standard uptake value is equivalent to the accumulation index.

Statistics

Data are presented as means and maximum error unless otherwise indicated. For significance tests, a paired two-sample Student's t-test ($\alpha < 0.05$) was applied after checking of similar parameter distribution by the Wilcoxon signed rank test ($\alpha < 0.05$).

RESULTS

Radiochemical Yield and In Vitro Immunoreactivity

The total radiochemical yield obtained after labeling and affinity purification of ^{76}Br-38S1 was 23% ± 5% in the three batches prepared for this study, resulting in a specific activity of 0.18 ± 0.07 MBq/μg. The labeling efficiency of ^{125}I to 38S1 was 84% ± 5%, resulting in a specific activity of 0.22 ± 0.02 MBq/μg. The in vitro immunoreactivity for ^{76}Br- and ^{125}I-38S1 was 80 ± 2% and 79 ± 3%, respectively.

Evaluation of MAb Kinetics and Biodistribution

The biodistribution of ^{76}Br and ^{125}I activity in tumor-bearing rats, evaluated at certain time points after injection of labeled 38S1, is presented as the average accumulation index (Fig. 1, Table 2).

In blood, the ^{76}Br concentration was higher than that of ^{125}I from 2 hr postinjection of labeled MAb 38S1 at all times of analysis (Fig. 1). The uptake in tumor xenografts located both in the flank and in the hind leg apparently reached maximum values 2 days after the administration of 38S1. The radioactivity concentrations in liver and other normal tissues were lower than that in tumors from Day 1 and onwards. Except for muscle and ^{125}I-activity in thyroid, normal tissue radioactivity decreased throughout the period, although at a relatively slower rate for ^{76}Br activity.

At all times of analysis the average accumulation index of ^{76}Br-activity in tumors was higher (14%–35%) than that of ^{125}I activity. However, this difference was also found, more pronounced, in most normal tissues. On Day 4, the percentage by which the ^{76}Br accumulation index exceeded that of ^{125}I ranged from 27% in tumors up to 320% in stomach (Table 2). In iodide-suppressed thyroid, however, more ^{125}I than ^{76}Br accumulated throughout the period. This was also the case in urine samples, where the ^{125}I concentrations during the first day were about threefold higher than the ^{76}Br concentrations. At later time points, the differences in urine were less significant. Apart from blood and ^{125}I in thyroid, the highest nontumor concentrations on Day four were found in bladder and lungs, and the lowest uptake in brain, for both ^{76}Br and ^{125}I activity.

TABLE 2
Mean Accumulation Index from Paired-Label Biodistribution of Bromine-76-38S1 and Iodine-125-38S1 or Bromine-76-79C and Iodine-125-79C 4 Days after MAb Administration

Tissue	^{76}Br-38S1	^{125}I-38S1	^{76}Br-79C	^{125}I-79C
Tumor	2.9 (0.8)	2.3 (1.1)	1.5 (0.9)	1.1 (0.8)
Blood	2.8 (0.4)	1.8 (0.3)	3.2 (0.2)	2.1 (0.2)
Kidney	0.86 (0.30)	0.36 (0.08)	1.0 (0.3)	0.51 (0.17)
Liver	0.84 (0.15)	0.51 (0.03)	1.0 (0.1)	0.93 (0.45)
Spleen	1.0 (0.24)	0.53 (0.11)	1.9 (0.2)	1.7 (0.6)
Pancreas	0.86 (0.30)	0.42 (0.02)	0.92 (0.31)	0.52 (0.31)
Stomach	1.0 (0.52)	0.23 (0.04)	1.3 (0.7)	0.48 (0.28)
Small intestine	0.56 (0.21)	0.19 (0.03)	0.64 (0.33)	0.30 (0.09)
Large intestine	0.89 (0.30)	0.35 (0.03)	0.81 (0.29)	0.31 (0.19)
Bladder	1.6 (0.4)	1.0 (0.3)	1.8 (0.5)	1.5 (0.7)
Heart	0.91 (0.38)	0.49 (0.07)	1.0 (0.3)	0.78 (0.35)
Lung	1.6 (0.5)	0.80 (0.06)	1.6 (0.3)	1.1 (0.4)
Muscle	0.48 (0.17)	0.24 (0.04)	0.36 (0.05)	0.24 (0.07)
Bone	0.62 (0.13)	0.23 (0.05)	0.34 (0.11)	0.23 (0.09)
Brain	0.26 (0.08)	0.07 (0.02)	0.29 (0.09)	0.07 (0.04)

Data are presented as mean (maximum variation) of samples from three animals.

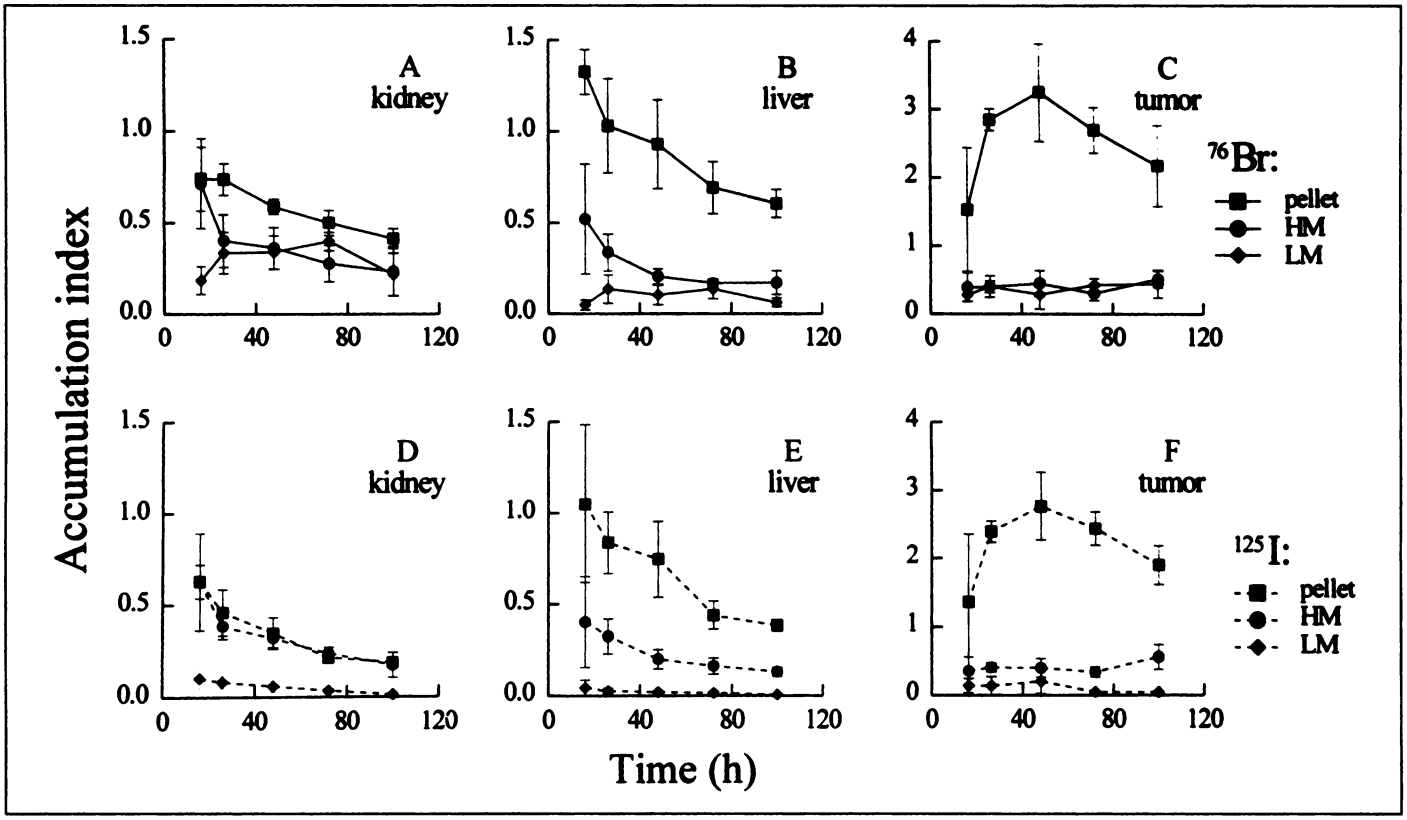

FIGURE 2. Fractionation of ^{76}Br and ^{125}I activity in tissue homogenates into pellets (squares), high molecular weight components (HM, circles) and low molecular weight components (LM, diamonds) over time after injection of ^{76}Br-38S1 and ^{125}I-38S1 (n = 3). (A-C) Bromine-76 activity in kidney, liver and tumors, respectively. (D-F) Iodine-125 activity in kidney, liver and tumors, respectively.

The normal tissue distribution of the nontumor-specific MAb 79C, 4 days after injection, agreed fairly closely with that of MAb 38S1 (Table 2). In spleen, stomach and liver, however, the accumulation of ^{125}I activity was at least twice as high for MAb 79C as for radioiodinated 38S1. The tumor concentration was, on average, about half that of the tumor-specific MAb 38S1.

Degradation of Radiohalogenated MAbs

In vitro, the radiobromine label and the radioiodine label were both found to be stable. After 4 days of incubation in human serum, 97% ± 1% of the total ^{76}Br activity and 96% ± 1% of total ^{125}I activity were bound to high molecular weight (HMW) components, representing protein-bound radioactivity. When blood samples were drawn from animals injected with ^{76}Br-38S1 and ^{125}I-38S1, the average plasma content of HMW ^{125}I activity was also high throughout the analysis, 97% ± 3%, whereas the corresponding figure for ^{76}Br activity was lower and more variable, 81% ± 16%.

Bromine-76 and ^{125}I activity values in pellet-, HMW-, and low molecular weight fractions from homogenates of tumors, kidneys and livers are displayed in Figure 2. The general pattern of radiolabel distribution in the tissue fractions was similar for ^{76}Br- and ^{125}I-activity. Particularly in tumors but also in livers, the bulk of the radioactivity was found in the pellet. When comparing the two radiolabels, the ^{76}Br concentration in the pellet fraction was higher than the ^{125}I concentration in tumors and all tissues. The concentration of HMW-bound radioactivity did not differ significantly ($p > 0.05$) between ^{76}Br and ^{125}I in the homogenized tissues, whereas LMW ^{76}Br activity was severalfold higher than LMW ^{125}I activity in all samples. The most prominent differences between these two radiolabels in both pellet and LMW fractions were found in the kidneys.

FPLC analysis showed that the low molecular weight radioactivity in blood and normal tissues was most probably in the form of free $^{76}Br^-$ and $^{125}I^-$ (Fig. 3), since the respective radiopeaks corresponded to reference halides (retention times 24 min and 38 min, bromide and iodide, respectively). In some cases, small peaks were found at the same retention time as bromotyrosine (27 min) and iodotyrosine (30 min). In addition,

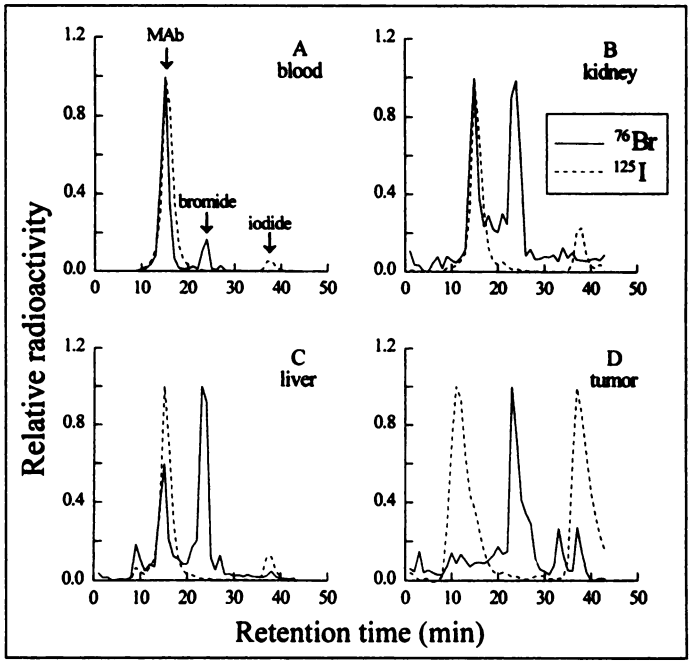

FIGURE 3. Radiochromatograms of ^{76}Br (line) and ^{125}I activity (dotted line) after FPLC-fractionation of blood plasma (A) and the supernatant from homogenized kidney (B), liver (C) and tumor (D), 27 hr after administration of ^{76}Br-38S1 and ^{125}I-38S1. The retention times of the reference compounds MAb 38S1, bromide and iodide was 15, 24 and 38 min, respectively.

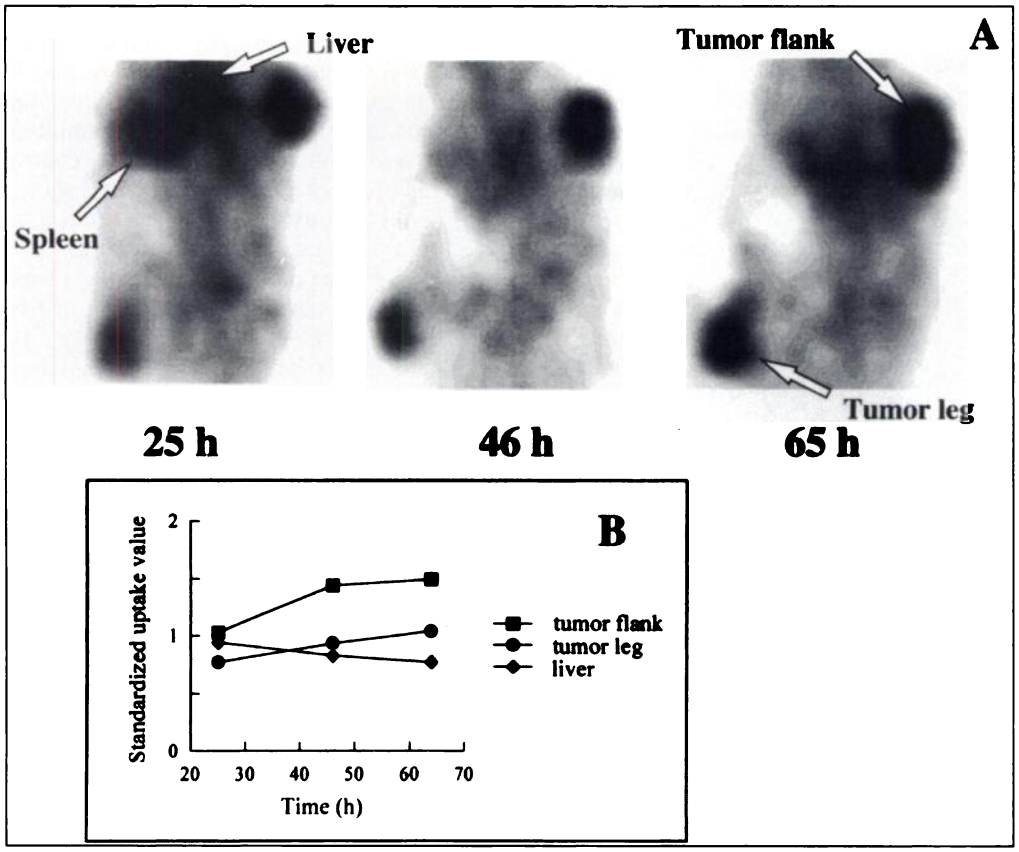

FIGURE 4. (A) PET images of ^{76}Br distribution in one rat after administration of ^{76}Br-labeled 38S1. All images show a coronal-sagittal section through both tumors and a part of the liver. (B) ROI measurements in the images shown in (A) of the flank tumor (squares), leg tumor (circles) and liver (diamonds).

the predominant HMW ^{76}Br and ^{125}I activity was eluted in fractions corresponding to intact radiolabeled MAb 38S1 (15 min). In homogenized tumors, however, the chromatograms were more difficult to interpret. A large part of the radioactivity, especially in the case of ^{76}Br, was found in the low molecular weight region. No ^{76}Br-MAb peak could be distinguished, and a significant amount of the ^{125}I activity was eluted in fractions corresponding to compounds of higher molecular weight than IgG-MAbs. Similar patterns were found when analyzing samples at the other time points of analysis.

Radioimmuno PET

In the PET images the tumor sites became more easily distinguishable over time due to the increasing tumor-to-tissue ratios; 14 of 16 tumor sites were readily discerned at 46 and 65 hr, and the uptake in the flank tumor was separable from liver uptake. All tumors weighing more than 0.5 g could be identified by PET. PET images of the distribution of ^{76}Br activity in one rat at various times postinjection of radiolabeled MAb 38S1 are shown in Figure 4 along with SUV calculations of tumors and liver. In the first image, obtained 25 hr postinjection, the highest concentrations of ^{76}Br activity was found in the tumors, liver and part of the upper abdominal region interpreted as the spleen. At later time points, the tumor uptake was predominant. In this rat, PET imaging revealed that the uptake of ^{76}Br increased in both tumors, and decreased in liver, during 3 days after MAb administration.

Kinetics and Biodistribution of Radiohalides

The blood concentration of ^{76}Br activity remained stable for days after the injection of radiohalides, and the clearance rate in tumors and normal tissues was low (Fig. 5, Table 3). In comparison to bromide, radioiodide was rapidly cleared from the blood, tumors and all normal tissues except presaturated thyroid (accumulation index 4.6 ± 0.7 on Day 2). On Day 2, the highest concentrations of ^{76}Br were found in the blood and spleen,

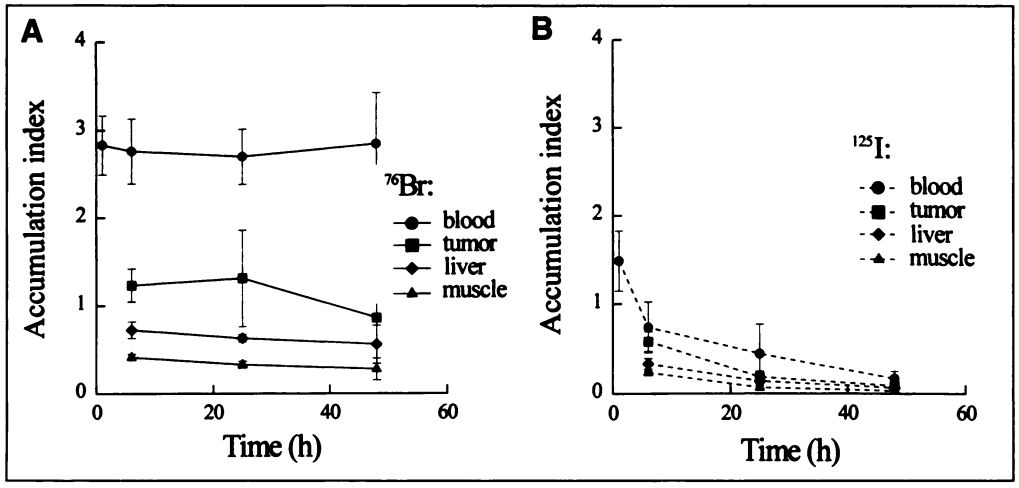

FIGURE 5. Accumulation index of ^{76}Br (A) and ^{125}I (B) halide ions over time. Blood samples (circles) were taken from 3–9 rats. Samples from tumors (squares), liver (diamonds) and muscle (triangles) were taken from three rats at each time point.

TABLE 3
Mean Accumulation Index from Paired-Label Biodistribution of $^{76}Br^-$ and $^{125}I^-$ 2 Days after Radiohalide Administration

Tissue	$^{76}Br^-$	$^{125}I^-$
Tumor	0.8 (0.4)	0.09 (0.09)
Blood	2.8 (0.6)	0.17 (0.09)
Kidney	0.9 (0.2)	0.09 (0.09)
Liver	0.6 (0.2)	0.06 (0.07)
Spleen	1.5 (0.1)	0.09 (0.07)
Pancreas	0.8 (0.2)	0.08 (0.07)
Stomach	1.2 (0.4)	0.4 (0.3)
Small intestine	0.7 (0.3)	0.10 (0.09)
Large intestine	0.8 (0.3)	0.16 (0.07)
Bladder	1.1 (0.4)	0.21 (0.13)
Heart	0.8 (0.2)	0.7 (0.5)
Lung	1.4 (0.3)	0.1 (0.09)
Muscle	0.3 (0.1)	0.03 (0.02)
Bone	0.5 (0.1)	0.07 (0.04)
Brain	0.3 (0.1)	0.009 (0.005)

Data are presented as mean (maximum variation) of samples from three animals.

whereas tumor uptake of $^{76}Br^-$ was intermediate. Thyroid accumulation of ^{76}Br activity was 0.9 ± 0.1 2 days postinjection.

DISCUSSION

In the present study, ^{76}Br-labeled anti-CEA MAbs were successfully applied for PET imaging of human colon cancer xenografts in nude rats, allowing identification of all tumors weighing 0.5 g or more. PET imaging also revealed that, in contrast to what was found in the measurements of dissected tumors, the ^{76}Br uptake in some tumors increased for several days after ^{76}Br-MAb 38S1 injection. However, quantification of MAb tumor uptake from measurements in the PET images may result in lower values than γ-counting of dissected tumors. Due to the partial volume effect, the radioactivity concentration in objects with a size comparable to, or smaller than, the PET resolution will be underestimated (*26*). With small experimental animals such as rats, an underestimation of ^{76}Br uptake in most experimental tumors and essentially all organs except liver may be expected.

The general pharmacokinetic pattern of ^{76}Br-38S1 was comparable with that of ^{125}I-38S1, although the clearance rate of ^{76}Br activity was slower than ^{125}I clearance in most cases. This resulted in an overall higher concentration of ^{76}Br in tumors, blood and all tissues except the thyroid. Other investigators comparing directly radiobrominated and radioiodinated proteins also found a higher radiobromine content in blood and tissues, caused by a slower clearance of protein-bound radiobromine activity (*18,24*).

To evaluate whether this was also the case in the present investigation, further analysis of ^{76}Br- and ^{125}I-labeled compounds in blood, kidneys, livers and tumors was made. The results were not in accordance with the previous studies, since the concentration of ^{76}Br activity bound to MAb was essentially equal to the concentration of ^{125}I-MAb. In addition, the hydrolysis rates of ^{76}Br- and ^{125}I-labeled 38S1 in vitro were similar, about 1% a day. This suggests that the difference between the total amounts of radiobromine and radioiodine in vivo was not due to a less stable ^{125}I-label but rather to differences in the processing of low molecular weight radioactive species after MAb catabolism.

Indeed, the concentration of low molecular weight ^{76}Br activity, mainly in the form of free bromide, was severalfold greater than the concentration of free ^{125}I after labeled 38S1 injection. Only a few percent of ^{125}I activity in blood plasma was found to be free iodide, whereas the average radiobromide content in plasma sometimes amounted to one-third of the total plasma ^{76}Br activity. Thus, the higher total ^{76}Br concentration in blood could be mainly attributed to free $^{76}Br^-$. In the control experiment where free radiohalides were injected, it was shown that the bromide ion had a low excretion rate in contrast to iodide, probably due to different excretion mechanisms.

Although the higher ^{76}Br concentration in kidneys, livers and tumors in part also could be explained by the presence of free radiobromide after MAb degradation, there was also more ^{76}Br associated with insoluble components in the homogenized tissues. Whether this observation represents a true phenomenon in which ^{76}Br-MAb or ^{76}Br-labeled catabolites to a higher degree remained attached to (or incorporated into) insoluble components such as cell membrane components in vivo, or whether the difference was caused by ^{76}Br activity trapped in the pellet fraction during in vitro processing, cannot be concluded.

Regarding the pathway by which radiolabeled antibodies are catabolized, cellular internalization and degradation of radiolabeled MAbs or other proteins has been reported to ultimately result in radiolabeled amino acids (*27,28*). Depending on the radiolabel on the amino acid, the compound is thereafter retained in the lysosomes (e.g., ^{111}In-DTPA-lysine) or excreted from the cells (e.g., [^{125}I]iodotyrosine). Since deiodination enzymes for iodotyrosine are present in many tissues, including kidney, liver and thyroid (*29*), free ^{125}I could be produced in these organs. In a study where the content of radioiodide in urine from patients injected with radioiodinated MAbs was analyzed, a variety of radioactive catabolites was found, including radioiodide and iodotyrosine, as well as other compounds (*30*). In the case of radiobrominated proteins, it remains to be established how intracellular or extracellular catabolism leads to the formation of free bromide or other low molecular weight catabolites.

The average tumor-to-tissue ratio 4 days after MAb administration, brain and blood excluded, was for ^{76}Br activity 3.6 ± 1.3 (mean ± s.d.), which was lower than the average ^{125}I ratio (6.7 ± 3.3) due to the relatively higher concentration of ^{76}Br activity in normal tissues than in tumors. However, the tumor uptake in the present study was significantly lower in comparison to other investigations of ^{125}I-38S1 (*20,21*) or ^{76}Br-38S1 (unpublished data), in spite of similar labeling methods, immunoreactivities and tumor models. The only methodological difference was the iodide presaturation of rat thyroids in this study, which, in fact, was observed by Zamora et al. (*31*) to reduce tumor antibody uptake by 40%. The mechanisms by which the intake of iodide salts could result in such effects are, to our knowledge, unknown.

In a possible clinical situation, ^{76}Br catabolites would probably cause a significant background radioactivity after degradation of brominated MAb. However, in the present experimental study, the low molecular weight ^{76}Br activity in blood could be identified as being mainly free $^{76}Br^-$. This might provide a means whereby allowance could be made for a large part of this background radioactivity. The use of bromide is an established method for measuring the volume of extracellular space (*32,33*). In radioimmunodiagnosis with ^{76}Br-labeled MAbs, a small amount of $^{76}Br^-$ could be injected before MAb administration and images of the distribution of free bromide at equilibrium obtained within a few hours. At the time of imaging of ^{76}Br-MAb distribution, the free radiobromide concentration in a blood sample could then be used to create PET images of

the ^{76}Br-MAb distribution, corrected for the contribution of free radiobromide. Although somewhat speculative, tumor-to-blood ratios could possibly be improved by such a method in the case of ^{76}Br-labeled MAbs.

The high-energy positrons emitted in the ^{76}Br decay and the slow kinetics of intact MAbs make ^{76}Br-MAb dosimetry an important consideration. Biodistribution data from small experimental animals cannot readily be extrapolated to humans, which may cause difficulties in predicting normal organ dosimetry. No exceptionally high uptake of ^{76}Br was found in normal tissues of the rat after administration of 76Br-38S1 MAbs, and the elimination time for the main catabolite $^{-76}$Br was slow. Probably, this also would be the case in human studies. Hence, a simple calculation model for whole-body dose was applied, assuming an even distribution of ^{76}Br activity in the body and an elimination time equal to the physical decay. Dosimetry data was taken from an ICRU publication (*34*), and the calculations were carried out according to the recommendations in this report. The effective dose equivalent after the administration of 100 MBq ^{76}Br-MAb to an adult male was estimated to be 27 mSv, about twice the estimated dose from the same amount of ^{111}In-labeled MAbs (14 mSv) in this model.

In the evaluation of $^{76}Br^{-}$ biodistribution after radiohalide administration, the ^{76}Br-activity concentration in the experimental tumors was found to be similar to many normal tissues and lower than that in spleen and lung. Since the main part of the blood pool had been removed by exsanguination before dissection, the ^{76}Br concentration should reflect the volume of the interstitial space in the tissues. These results therefore indicate that the tumor interstitial volume was similar to, or smaller than, that in many normal tissues, which is contradictory to other investigations (*35*). Further studies, in larger animals or in man, are required to demonstrate whether the bromide distribution space reflects the interstitial space in tumors.

CONCLUSION

Bromine-76 is a potential radiolabel for PET imaging using monoclonal antibodies directed against tumor antigens. PET imaging of the ^{76}Br-labeled anti-CEA MAb 38S1 allowed identification of xenografts of human colorectal carcinoma in nude rats. No significant differences regarding the rate of dehalogenation of ^{76}Br-38S1 or ^{125}I-38S1 were found, but MAb catabolism resulted in high amounts of free radiobromide, which had a slow excretion rate in comparison with iodide. Therefore, the concentration of ^{76}Br activity was higher than the corresponding ^{125}I concentration in tumors, in blood and in most normal tissues.

ACKNOWLEDGMENTS

We thank Ms. Veronica Asplund for valuable technical assistance. Financial support was given by The Swedish Society for Cancer Research, grant 2971-B93-04XAB, The Swedish Medical Research Council, grant B94-39X-10888-01A and The Royal Swedish Academy of Sciences.

REFERENCES

1. Garg PK, Garg S, Bigner DD, Zalutsky MR. Localization of fluorine-18-labeled Mel-14 monoclonal antibody F(ab')$_2$ fragment in a subcutaneous xenograft model. *Cancer Res* 1992;52:5054–5060.
2. Otsuka FL, Welch MJ, Kilbourn MR, et al. Antibody fragments labeled with fluorine-18 and gallium-68: in vivo comparison with indium-111 and iodine-125-labeled fragments. *Nucl Med Biol* 1991;18:813–816.
3. Page RL, Garg PK, Garg S, Archer GE, Bruland ØS, Zalutsky MR. PET imaging of osteosarcoma in dogs using a fluorine-18-labeled monoclonal antibody Fab fragment. *J Nucl Med* 194;35:1506–1513.
4. Vaidyanathan G, Bigner DD, Zalutsky MR. Fluorine-18-labeled monoclonal antibody fragments: a potential approach for combining radioimmunoscintigraphy and positron emission tomography. *J Nucl Med* 1992;33:1535–1541.
5. Goethals P, Coene M, Slegers G, et al. Production of carrier-free ^{66}Ga and labeling of antimyosin antibody for positron imaging of acute myocardial infarction. *Eur J Nucl Med* 1990;16:237–240.
6. Anderson CJ, Connett JM, Schwarz SW, et al. Copper-64-labeled antibodies for PET imaging. *J Nucl Med* 1992;33:1685–1691.
7. Lövqvist A, Sundin A, Ahlström H, Carlsson J, Lundqvist H. Bromine-76-labeled monoclonal anti-CEA antibodies for radioimmuno positron emission tomography. *Nucl Med Biol* 1995;22:125–131.
8. Srivastava SC, Mausner LF, Kolsky, et al. In: Jones JR, Pichat L, Wolf A, eds. *Production and use of cobalt-55 as an antibody label for PET imaging* [Abstract]. *J Labeled Compd Radiopharm* 1994;35:389–390.
9. Bakir MA, Eccles SA, Babich JW, et al. c-erbB2 overexpression in breast cancer as a target for PET using iodine-124-labeled monoclonal antibodies. *J Nucl Med* 1992;33: 2154–2160.
10. Daghighian F, Pentlow KS, Larson SM, et al. Development of a method to measure kinetics of radiolabeled monoclonal antibody in a human tumor with applications to microdosimetry: PET studies if iodine-124-labeled 3F8 monoclonal antibody in glioma. *Eur J Nucl Med* 1993;20:402–409.
11. Larson SM, Pentlow KS, Volkow ND, et al. PET scanning of iodine-124-3F9 as an approach to tumor dosimetry during treatment planning for radioimmunotherapy in a child with neuroblastoma. *J Nucl Med* 1992;33:2020–2023.
12. Pentlow KS, Graham MC, Lambrecht RM, Cheung N-KV, Larson SM. Quantitative imaging of iodine-124 using positron emission tomography with applications to radioimmunodiagnosis and radioimmunotherapy. *Med Phys* 1991;18:357–366.
13. Rubin SC, Kairemo KJA, Brownell A-L, et al. High-resolution positron emission tomography of human ovarian cancer in nude rats using ^{124}I-labeled monoclonal antibodies. *Gynecol Oncol* 1993;48:61–67.
14. Westera G, Reist HW, Buchenegger F, et al. Radioimmuno positron emission tomography with monoclonal antibodies: a new approach to quantifying in vivo tumor concentration and biodistribution for radioimmunotherapy. *Nucl Med Commun* 1991; 12:429–437.
15. Wilson CB, Snook DE, Dhokia B, et al. Quantitative measurement of monoclonal antibody distribution and blood flow using positron emission tomography and ^{124}I in patients with breast cancer. *Int J Cancer* 1991;47:344–347.
16. Mazière B, Loc'h C. Bromine radiopharmaceuticals: radiopharmaceuticals labeled with bromine isotopes. *Appl Radiat Isot* 1986;37:703–713.
17. Manthey JA, Hager LP. Characterization of the catalytic properties of bromoperoxidase. *Biochemistry* 1989;28:3053–3057.
18. McElvany KD, Welch MJ. Characterization of bromine-77-labeled proteins prepared using bromoperoxidase. *J Nucl Med* 1980;21:953–960.
19. Lambert F, Slegers G, Goethals P. Preparation of bromine-77-labeled monoclonal anti-hPLAP antibody using chloramine-T. *J Labeled Compd Radiopharm* 1991;29: 729–737.
20. Ahlström H, Carlsson L, Hedin A, Lörelius LE. An experimental model for pharmacokinetic studies of monoclonal antibodies in human colonic cancer. *Acta Oncol* 1987;26:1–5.
21. Sundin A, Ahlström H, Carlsson L, Graf W, Glimelius B, Carlsson J. Radioimmuno localization of hepatic metastases and subcutaneous xenografts from a human colonic cancer in the nude rat: aspects of tumor implantation site and mode of antibody administration. *Acta Oncol* 1993;32:877–885.
22. Hedin A, Hammarström S, Larsson Å. Specificities and binding properties of eight monoclonal antibodies against carcinoembryonic antigen. *Mol Immunol* 1982;19: 1641–1648.
23. De Jesus OT, Mukherjee J, Khalifah RG. Synthesis of radiobrominated m-tyrosine. *J Labeled Comp Radiopharm* 1989;27:189–194.
24. Scott-Robson S, Capala J, Carlsson J, Malmborg P, Lundqvist H. Distribution and stability in the rat of a ^{76}Br/^{125}I-labeled polypeptide, epidermal growth factor. *Nucl Med Biol* 1991;18:241–246.
25. Tom BH, Rutzky LP, Jakstys MM, Oyasu R, Kaye CI, Kahan BH. Human colonic adenocarcinoma cells. 1. Establishment and description of a new line. *In Vitro* 1976;12:180–191.
26. Litton JE, Bergström M, Eriksson L, Bohm C, Blomqvist G, Kesselberg M. Performance study of the PC-384 positron camera system for positron emission tomography of the brain. *J Comput Assist Tomogr* 1983;8:74–87.
27. Geissler F, Anderson SK, Venkatesan P, Press O. Intracellular catabolism of radiolabeled anti-μ antibodies by malignant B-cells. *Cancer Res* 1992;52:2907–2915.
28. Duncan JR, Welch MR. Intracellular metabolism of indium-111-DTPA-labeled receptor targeted proteins. *J Nucl Med* 1993;34:1728–1738.
29. Stanbury JB, Morris ML. Deiodination of diiodotyrosine by cell-free systems. *J Biol Chem* 1958;233:106–108.
30. DeNardo GL, DeNardo SJ, Miyao NP, et al. Non-dehalogenation mechanisms for excretion of radioiodine after administration of labeled antibodies. *Int J Biol Markers* 1988;3:1–9.
31. Zamora PO, Pant KD, Shah VO, et al. Anti-colon/ovarian tumor antigen: localization of colon cancer xenografts in athymic mice. *Nucl Med Biol* 1988;15:261–270.
32. Blahd WH. Radioisotope techniques. In: Maxwell MH, Kleeman CR, eds. *Clinical disorders of fluid and electrolyte metabolism*. McGraw-Hill; 1972:613–627.
33. Nicholson JP, Zilva JF. Estimation of extracellular fluid volume using radiobromine. *Clin Sci* 1960;19:391–398.
34. International Commission on Radiation Units, Measurements. Methods of assessment of absorbed dose in clinical use of radionuclides. *ICRU Report* 1979.
35. Jain RK. Transport of molecules in the tumor interstitium: a review. *Cancer Res* 1987;47:3039–3051.